ORIGINAL RESEARCH ARTICLE

A New Parameter of Growth Inhibition for Cell Proliferation Assays[†]

Francesco Paolo Fiorentino [1,2,‡,*] Luigi Bagella[2,3], and Irene Marchesi [1,‡,*]

[1]Kitos Biotech Srls, Tramariglio, 07041 Alghero (SS), Italy.
[2]Department of Biomedical Sciences, University of Sassari, Sassari 07100, Italy.
[3]Sbarro Institute for Cancer Research and Molecular Medicine, Center for Biotechnology, College of Science and Technology, Temple University, Philadelphia, PA 19122, USA.

*****Both F.P.F.and I.M. are corresponding authors. F.P.F. email: fpfiorentino@gmail.com; I.M. email: iremarchesi@gmail.com

[†]This article has been accepted for publication and undergone full peer review but has not been through the copyediting, typesetting, pagination and proofreading process, which may lead to differences between this version and the Version of Record. Please cite this article as doi: [10.1002/jcp.26208]

Additional Supporting Information may be found in the online version of this article.

Received 25 August 2017; Accepted 3 October 2017
Journal of Cellular Physiology

DOI 10.1002/jcp.26208

ABSTRACT

Cell proliferation assays are performed by four decades to test the anti-proliferative activity of natural products and synthetic compounds in cell cultures. In cancer research, they are widely employed to evaluate drug efficacy in *in vitro* tumor models, such as established cell lines, primary cultures and recently developed three-dimensional tumor organoids. In this manuscript, we demonstrated that current employed parameters used by researchers to quantify *in vitro* growth inhibition, IC_{50} and GI_{50}, lead to a misinterpretation of results based on the exponential, and not linear, proliferation of the cells in culture. Therefore, we introduce a new parameter for the analysis of growth inhibition in cell proliferation assays, termed relative population doubling capacity, that can be employed to properly quantify the anti-proliferative activity of tested compounds and to compare drug efficacy between distinct cell models.

Keywords:
Cytotoxicity, Cell Proliferation, Cell Viability, Drug Toxicity, Drug screening

This article is protected by copyright. All rights reserved

INTRODUCTION

Cell proliferation assays are an extensively employed tool to evaluate the efficacy of tested compounds on a biological *ex vivo* model of interest. In anticancer drug development, they are used to evaluate the anti-proliferative activity of tested compounds on established tumor cell lines, primary tumor cells and 3D tumor organoids (Adan et al., 2016; Finlay and Baguley, 1984; Horvath et al., 2016; Moffat et al., 2014; Boyd:1992ht Rello-Varona et al., 2015; Selby et al., 2017). In a typical assay, cells are plated on a culture vessel and, after a sufficient amount of time necessary to recover growing phase, tested compounds are added to culture medium. At arbitrary chosen time-points, the number of cells is estimated by cell count or by an indirect method, such as measuring DNA synthesis, lactate-pyruvate conversion or ATP concentration (Barone et al., 2017; Fiorentino et al., 2016; Kato et al., 2016; Marchesi et al., 2017; Nieddu et al., 2016; Pau et al., 2009). A parameter, representative of drug efficacy, is subsequently calculated for data representation. In this manuscript, we first describe the two most employed parameters to analyze raw data and represent *in vitro* drug efficacy: the relative cell number (R), used to calculate the half maximal inhibitory concentration (IC_{50}), and the percentage of growth (PG), with an highlight on their limitations (Boyd and Paull, 1995; Yoshida et al., 1975). We emphasize that, using these parameters to compare drug efficacy between distinct cell populations (such as cell lines), cells that grow "faster" in culture will be inferred more sensitive than "slower" ones, and therefore these parameters lead to a misinterpretation of the results because of their dependency to the unique growth properties of each cell population. Despite PG partially overcomes this limitation, we provide in the first section of the results a detailed description of the dependency of R, and consequently the IC_{50}, to cell proliferation rate because of its frequent usage in current anticancer drug discovery research (as few recent examples (Ben Jannet et al., 2017; Cabrera et al., 2017; Esposito et al., 2017; Hamed et al., 2017; Indovina et al., 2017; Koul et al., 2017; Mathema et al., 2017; Menderes et al., 2017; Mukunthan et al., 2017; Muñoz et al., 2017; Potenza et al., 2017; Ravi et al., 2017; Rimoldi et al., 2017; Said et al., 2017; Venkataramana Reddy et al., 2017; Wehbe et al., 2017; Zamora et al., 2017; Zhu et al., 2017)). Subsequently, in the second section of the results, we show that PG is also dependent on the growth properties of the cells, because of their exponential and not linear proliferation in culture. Therefore,

we introduce a new parameter to determine growth inhibition, the relative doubling capacity (RD), that can be used to properly quantify and compare the anti-proliferative activity of tested compounds on exponential growing cell models.

MATERIALS AND METHODS

Cell cultures

Lung adenocarcinoma A549 and prostate adenocarcinoma PC3 cell lines were obtained from cell bank of the IRCCS University Hospital San Martino – IST National Institute for Cancer Research (Genova, Italy). Cells were cultured in DMEM supplemented with L-Glutamine and 10% FBS (Lifetech) at 37°C, 5% CO_2 humidified air.

Kinetics of Cell Proliferation

500 A549 cells suspended in 20 µL of complete culture medium without phenol red were plated in 384 well flat, clear bottom black microplate (Corning #3764). After 18-24 hours, 10 µL of fresh supplemented culture medium, containing Etoposide (Sigma-Aldrich #E2600000), SiR-Hoechst (Spirochrome #SC007) (Lukinavičius et al., 2015) and CellTox™ Green Dye (Promega #G873A), were added to each well of the cell plate, to a final concentration of SiR-Hoechst 0.5µM in vehicle (DMSO) 0.8%. A549 cells were treated with eleven 1:2 serial dilutions of Etoposide in technical triplicate, ranging from 40 µM to 40 nM. Plating of cells, preparation of Etoposide serial dilutions and addition of compound solutions to the cells were performed using an automated liquid handling platform (Gilson Pipetmax®). Multiple live-cell imaging in far-red fluorescence (led cube 625 nm, filter cube excitation 650 ± 30 nm, emission 800 ± 90 nm), green fluorescence (led cube 465 nm, filter cube excitation 469 ± 25 nm, emission 525 ± 25 nm) and phase contrast was performed at 37°C, 5% CO_2 using a gas controller associated to the microscope, after 1, 24, 48 and 72 hours of treatment with a 4x objective, using an automated digital widefield microscope (BioTek Cytation 5). For each sample, four images were taken to cover the entire area of the well. Image merging, processing and cell count were performed using BioTek Gen5 software. Briefly, the number of cells

was calculated as count of far-red fluorescence stained nuclei and the number of dead cells was calculated as count of green fluorescence stained cells. Threshold of fluorescence background and range of nuclei size settings were manually adjusted in each experiment by overlapping images of far-red and green fluorescence with images in phase contrast as reference. Count of live cells was calculated by subtracting count of dead cells to the count of total cells. For what concerns cytotoxicity assays in PC3 cells, 2000 cells suspended in 80 µL of complete culture medium without phenol red were plated in 96 well flat, clear bottom black microplate (Corning #3603). After 18-24 hours, 20 µL of fresh supplemented culture medium, prepared as previously described for A549 cells, was added to each well of the cell plate. PC3 cells were treated with nine 1:2 serial dilutions ranging from 10 µM to 40 nM in technical duplicate. Live-cell imaging and analysis were performed as previously described.

Statistical analysis.

Regression analysis and T-tests were performed with microsoft excel.

RESULTS

The Relative Cell Number is Function of Cell Proliferation

R is a widely used parameter to determine drug efficacy in cell proliferation assays, and it is also used to calculate the IC_{50} and compare drug efficacy between distinct cell models. R can be described as:

(1) $$R = {}^{T}/_{U} \cdot 100$$

where T is number of cells at the measuring point in the compound-treated sample and U is number of cells in the untreated control sample. R has a value from “0”, which means maximum drug efficacy, to “100”, which means absence of any effect by the treatment on cell proliferation. However, cell populations that grow “faster” in culture, referring to cells that duplicate more times in the same

amount of time than “slower” ones, tend to show lower R. This logical deduction can be assumed if we imagine to treat two distinct cell lines (A and B) with a drug that induces total arrest of cell growth, termed cytostasis, in both cell lines (Figure 1A). Despite the same phenotype is induced in both cell lines, R_A of the “faster” cell line A will be lower than R_B of the “slower” cell line B, and therefore A will be inferred more sensitive than B when comparing drug efficacy between the two cell lines. For the same reason, R is function of the period of treatment before estimation of cell number: if we treat a cell line with cytostatic doses of a drug and estimate the number of cells at distinct time points, R logically tends to show lower values at longer period of treatment because of the increased cell number in untreated sample, independently by additive drug effects due to longer exposition (Figure 1B). To experimentally evaluate these assumptions, we treated a representative cell line, A549, with serial dilutions of a well-characterized representative chemotherapy agent, etoposide, and live cell number was monitored every 24 hours for three days (Figure 2). A preliminary normalization of cell number among wells at each time point was carried out taking advantage of the multiple readings with live-cell imaging:

$$Normalized\ number\ of\ cells\ in\ well\ x\ at\ time\ point\ y: \frac{Number\ of\ cells\ in\ well\ x\ at\ time\ point\ y}{Number\ of\ cells\ in\ well\ x\ after\ 1\ hour\ of\ treatment}$$

Subsequently, R and IC_{50} were calculated using normalized data at each time point (Supplemental Data S1 and Table 1, respectively). A much higher coefficient of variation was observed in the IC_{50} at 24 hour compared to 48 and 72 hours of treatment (Table 1). Since a concomitant higher coefficient of variation in the proliferation of untreated cells was not observed (Table 1), we concluded that tiny differences in drug concentration and timing of data collection among the biological replicates would strongly affect drug efficacy at a short time of treatment, as 24 hour. Therefore, we compared R and IC_{50} values between 48 and 72 hours of treatment. As shown in Figure 1C, R values after 72 hours of treatment were lower than those obtained at 48 hours. Consistently, IC_{50} after 72 hours of treatment was significantly lower than IC_{50} at 48 hours (Table 1, $p<0.01$, two-tail heteroscedastic t-test). Similar results were obtained using a different set of data originated by treatment of PC3 cells with serial dilutions of etoposide (Table 2, Figure 1D and

Supplemental Data S2). Despite it could be argued that lower R at 72 hours of treatment could be partially or totally due to the longer exposure of cells to the drug, we showed that R is function of cell proliferation rate, suggesting that R would not be a proper parameter to determine drug efficacy in cell proliferation assays, if the aim is to compare drug sensitivity between cell lines with distinct proliferation rates.

The Percentage of Growth Inhibition is Function of Cell Proliferation

Researchers at the NCI's Drug Discovery Program developed, more than 20 years ago, a parameter to compare efficacy of small molecules with potential anticancer activity in a panel of 60 tumor cell lines, which is still used in their program (Boyd et al., 1992). Cell number is estimated at the time of compound addition and after 48 or 72 hours of treatment, and efficacy is determined as percentage of growth (PG). PG is differently calculated based on the type of effect: percentage of cell death (PG_T) if a cytotoxic effect occurs, or percentage of growth inhibition (PG_S) if a decrement of cell proliferation or cytostasis occurs. PG_T and PG_S are described as:

(2) $$PG_T = \frac{T-I}{I} \cdot 100$$

(3) $$PG_S = \frac{T-I}{U-I} \cdot 100$$

where I is the number of cells measured at the time of drug addition to cells. PG has a value from +100 to -100 and it is used to determine three response parameters: 50% growth inhibition (GI_{50}, PG=50), total growth inhibition (TGI, PG=0) and lethal concentration 50% (LC_{50}, PG=-50) (Boyd and Paull, 1995). First, PG is a more informative parameter than R to evaluate *in vitro* drug efficacy since it distinguishes among growth inhibition and cytotoxic effects. PG_T describes the percentage of cells that die as a consequence of the treatment, and therefore it does not take into account the proliferation rate in untreated cells. In the same manner, if cytostasis occurs, PG_S is "0" regardless

of cell proliferation properties. In contrast, if a partial growth inhibition occurs, PG_S is calculated as the percentage of linear increase in the number of treated cells to the linear increase in the number of untreated cells. As a consequence, PG_S will be function of cell proliferation if cell proliferation shows a non-linear progression (Figure 3A). To experimentally evaluate PG dependency to cell proliferation rate, we calculated PG, GI_{50} and TGI of previously used data of etoposide-treated A549 and PC3 cells. PG values in A549 cells after 72 hours of treatment were lower than PG values obtained after 48 hours for drug doses that induced growth inhibition (Figure 3B, right top quadrant). Consistently, GI_{50} after 72 hours of etoposide treatment in A549 cells was lower than GI_{50} after 48 hours, despite with lesser extent than IC_{50} values (Table 1, $p<0.05$, two-tail heteroscedastic t-test). We did not observe any difference in PG values for drug doses that induced a cytostatic (PG ~0) or a cytotoxic (PG < 0) effect (Figure 3B, in proximity of 0 values and left bottom quadrant, respectively). Consistently, the TGI concentration did not significantly differ between 48 and 72 hours of treatment in A549 cells (Table 1). This latter fact supports our hypothesis that both R and PG_S decrements at 72 hours of treatment are consequence of the increased cell number in untreated sample, and not of the longer drug exposure, otherwise a PG decrement would be observed also for drug doses that induced a cytostatic or cytotoxic effect (Figure 3B). For what concerns PC3 cells, GI_{50} and PG_s at 72 hours of treatment showed a slighter, not significant change between 48 and 72 hours of treatment (Table 2, Figure 3C and Supplemental Data S2).

Untreated Cell Populations Cultivated Under Standard Conditions Grow in an Exponential Manner

We hypothesized that the occurrence of an exponential, and not linear, growth of untreated A549 cells would contribute to the gradual PG_S decrement over the time of treatment in this cell line. This hypothesis was based on the logical assumption that each mother cell duplicates into two daughter cells, which will duplicate into two new cells and so on. To evaluate which mode of growth, linear or exponential, best fits cells maintained under standard culture conditions, we performed both linear and exponential regression analyses to the previously used data of untreated A549 and PC3

cells and calculated their coefficients of determination (R^2) (Figure 4A and Supplemental Data S3). The exponential regression of the growth curves of untreated A549 samples showed a R^2>0.99 in all the three biological replicates performed, whereas the linear regression showed a R^2<0.95. In PC3 cells, both the exponential and the linear regression analyses showed a R^2>0.95, with a slight higher R^2 in the exponential one. It was likely that the slighter, not significant difference of GI_{50} in PC3 cells between the two time-points was due to the growth properties of this cell line, whose fit both a linear and an exponential regression analysis in standard culture conditions. In contrast, our results confirmed that A549 cells grew in an exponential manner, and the PG_S decrement observed between 48 and 72 hours of etoposide treatment could be explained by the non-linear proliferation of untreated samples in this cell line.

We next asked if a model of exponential growth would better fit also growth curves of etoposide-treated samples (Supplemental Data 4). We arbitrary partitioned data into milder and stronger growth inhibition effects, using PG_S 35 as cut-off value, to evaluate more in detail the effects of growth inhibition on the proliferation property of the cells. Samples treated with doses of drug that induced a milder growth inhibition (PG>35) showed similar R^2 values of untreated cells in both cell lines, and therefore we concluded that a mild growth inhibition does not affect the growth properties of the cells (Figures 4B and 4C). In contrast, both regression analyses showed low R^2 values in samples that induced a stronger growth inhibition (0<PG<35), and no difference between linear and exponential R^2 values were observed (Figure 4B and 4C). Therefore, we concluded that a strong growth inhibition negatively affect the exponential growth of the cells. Overall, we confirmed that proliferation in untreated samples, in particular A549 cells, better fit a model of exponential growth and that this growth property is negatively affected by drug treatment, in particular for drug doses that induce a strong growth inhibition. We therefore speculated that PG_S decrement between 48 and 72 hours of etoposide treatment, shown in Figure 3B, was consequence of the exponential growth property of the cells.

The Relative Doubling Parameter Determines Growth Inhibition of Exponential Growing Cell Populations

Based on our previous observations and conclusions, we defined a parameter of drug efficacy representative of the residual exponential growth in treated cell populations. Taking into account that each cell duplicates into two daughter cells, number of cells in an untreated population at any time point can be described as:

(4) $$U = I \cdot 2^P$$

where P is the number of population doublings that an asynchronous cell population accomplished in a defined period of time. Therefore, population doublings can be described as:

(5) $$P = \log_2 \frac{U}{I}$$

Based on the hypothesis that growth inhibition is consequence of the impaired cell population doubling performance induced by the treatment, and therefore capacity of cell duplication, number of cells in a treated population (T) can be described as:

(6) $$T = I \cdot (D + 1)^P$$

where D, the doubling capacity, is between +1 and 0 and can consequently be described as:

(7) $$D = \sqrt[P]{T/I} - 1$$

To calculate the efficacy of treatment to impair the doubling capacity of the cell population, the number of population doublings accomplished by untreated cells was applied to treated sample. RD can be described as:

(8) $$RD = \sqrt[\log_2 U/I]{T/I} - 1 \cdot 100$$

Whereas PG_S is the relative linear growth of treated sample to the linear growth of untreated sample, RD can be described as the doubling capacity of treated sample to the doubling capacity of untreated sample. As for R and PG_S, RD has a value from 0 to 100 and can be used as well to determine two response parameters: 50% doubling capacity inhibition (RD_{50}, RD=50) and total doubling capacity inhibition, which corresponds to cytostasis as for TGI (RD_0, RD=0). We calculated RD, RD_{50} and RD_0 of etoposide-treated A549 and PC3 cells using previously used data of etoposide treatment. In Figures 5A and 5C we show RD at 48 and 72 hours of treatment, in addition to PG_S values as previously shown in Figures 3B and 3C, and in Figures 5C and 5D we provide a more detailed analysis by reporting the decrements of RD and PGs between 48 and 72 hours of treatment. In both cell lines, the decrement at 72 hours compared to 48 hours of treatment observed in PG_S values was strikingly reduced in RD values. Consistently, the decrement of RD_{50} at 72 hours, compared to 48 hours, was significantly less pronounced than GI_{50} decrement in both cell lines (Table 1 and Table 2, $p<0.01$ and $p<0.05$ in A549 and PC3 cells, respectively. One-tail paired t-test). As expected, we did not observe significant differences between TGI and RD_0 in A549 cells, since the value is "0" in both parameters regardless of cell proliferation (Table 1). These results confirmed that a parameter that measures the ability to negatively affect the doubling capacity of cell populations is more accurate than PG_S to represent *in vitro* growth inhibition, since it is not affected by the exponential growth property of cells in culture. We invite researchers to employ RD in their studies to confirm our conclusion with their own data and to properly compare drug efficacy between distinct cell models.

DISCUSSION AND CONCLUSIONS

Cell proliferation assays are routinely performed to evaluate *in vitro* efficacy of tested compounds in anticancer drug discovery research. Relative cell number (R) and percentage of growth (PG) are parameters widely employed by researchers to show the efficacy of tested compounds on the proliferation of cells in culture because of their simplicity and intuitiveness (Boyd and Paull, 1995; Yoshida et al., 1975). However, here we show here that both parameters are function of cell proliferation in tested cell model (Figure 1 and Figure 3). In order to experimentally evaluate our hypothesis, we treated two representative cell lines with a well-known chemotherapy agent, etoposide, and employed live-cell imaging technique to monitor the number of cells at several times of treatment (Figure 2). We also show here that PG_S dependency to cell proliferation is due to the exponential, and not linear, growth of cell in culture (Figure 4). As consequence, a drug that shows a high R or PG_S value after 48 hours of treatment could show lower values after longer period of treatment because of the increased growth of untreated cells and not the putative additive effects of the drug. As another example, a cell line with a fast proliferation rate in culture would show lower R or PG_S values than a "slower" cell line and would be inferred more sensitive to a drug when comparing drug efficacy between the two cell lines. This is of particular relevance in studies that compare drug efficacy in distinct cell models, as cell lines, with distinct growth properties. For instance, non-tumor cells, which usually tend to duplicate slower than the tumor counterpart, shows higher IC_{50} and GI_{50} values than tumor cells and could be misinterpreted as less sensitivity to tested compounds. Same misinterpretation could occur in studies of personalized medicine that associate drug sensitivity to genetic mutations or expression profiles, since higher sensitivity will be attributed to faster growing cell lines independently by their genome or transcriptome profiles. Therefore, the development of a more precise and refined method of analysis of proliferation assays would let researchers to better pick up drug candidates for further analysis, and ultimately provide more predictable results to *in vivo* tests. In our representative experiments, the exponential growth of cells was negatively affected by drug treatment (Figure 4). We therefore developed a new parameter of drug efficacy, termed relative doubling capacity (RD), which quantifies the impairment of doubling capacity consequence of drug treatment. RD is a more reliable parameter than PG_S to properly

compare drug efficacy because it is less, or none, affected by the unique growth properties of cells in culture (Figure 5, Table 1 and Table 2).

Despite it could be argued that the desired endpoint of antitumor preclinical drug discovery studies is to induce massive cell death and therefore the LC_{50} parameter, which quantifies drug toxicity, is the most relevant parameter for *in vitro* tests, we believe that the proper determination of growth inhibition is relevant as well. Indeed, the quantification of growth inhibition is relevant to define side effects on non-tumor cells or on tumor cells that do not carry the genetic alteration targeted by the tested compounds in studies of personalized medicine, or to evaluate effects on proliferation by compounds that are designed to target other cancer-related phenotypes, such as dedifferentiation or metastatization. We therefore invite other researchers to employ RD in their studies, together with PG_T, to properly determine *in vitro* drug efficacy of tested compounds.

DECLARATIONS:

ACKNOWLEDGMENT

F.P.F. acknowledges the support from Fondazione Umberto Veronesi (Postdoctoral Grant 2017).

COMPETING INTERESTS

The authors declare no conflicts of interest.

ABBREVIATIONS

R, Relative Cell number
PG, Percentage of Growth
PG_S, Percentage of Growth Inhibition
PG_T, Percentage of Cell Death
RD, Relative Doubling Capacity.

FIGURE LEGENDS

Figure 1. R is function of cell proliferation rate. (A) Cell line A and cell line B are treated with a drug at a concentration that induces total growth inhibition in both cell lines. Cell number is measured at time point t. Relative cell number of A, R_A, is 25 and relative cell number of B, R_B, is 50. **(B)** A cell line is treated at t_0 with a drug at a concentration that induces cytostasis. Two representative time points after compound addition were chosen to estimate cell number, t_1 and t_2, where $t_1 - t_0 = t_2 - t_1$. Relative cell number at t_1, R_1, is 50 and relative cell number at t_2, R_2, is 25. **(C, D)** Relative cell number of etoposide-treated A549 (C) or PC3 (D) cells after 48 and 72 hours of treatment. Each point refers to R values calculated from each technical replicate of the three biological replicates.

Figure 2. Representative time course of treatment of A549 with serial dilutions of etoposide. Multiple live-cell imaging was carried out 30 minutes, 24, 48 and 72 hours after drug addition to cells. Nuclei of cells were stained in far-red fluorescence by SiR-Hoechst and nuclei of dead cells were highlighted in green fluorescence by Promega CellTox staining. Cell number at each time point was estimated by counting red nuclei without positive green fluorescence signal.

Figure 3. PG is function of cell proliferation rate. (A) A cell line is treated at t_0 with a drug at a concentration that induces a 50% cell growth reduction. Two representative time points after compound addition were chosen to estimate cell number, t_1 and t_2, where $t_1 - t_0 = t_2 - t_1$. PG_{S1} at t_1, is 50 and PG_{S2} at t_2 is equal to PG_{S1} exclusively if cell growth progresses in a linear manner. **(B, C)** Percentage of growth inhibition of A549 (B) or PC3 (C) cells after 48 and 72 hours of etoposide treatment. Each point refers to R values calculated from each technical replicate of the three biological replicates.

Figure 4. Drug treatment negatively affects the exponential growth of cells. (A) R^2 calculated from linear or exponential regression analyses of growth curves of untreated A549 or PC3 cells. Each point is a biological replicate of the cell proliferation assay. **(B, C)** R^2 calculated from regression

analyses of growth curves of etoposide-treated A549 (B) or PC3 (C) cells that resulted in growth inhibition.

Figure 5. RD shows reduced variability than PG between 48 and 72 hours of treatment. (A, B) Relative doubling capacity and percentage of growth inhibition in A549 (A) or PC3 (B) cells after 48 and 72 hours of etoposide treatment. **(C, D)** Dispersion plot of RD and PG decrements (72 hours minus 48 hours of treatment) for doses of drug that induced growth inhibition in A549 (C) or PC3 (D) cells.

REFERENCES

Adan, A., Kiraz, Y., and Baran, Y. (2016). Cell Proliferation and Cytotoxicity Assays. Curr Pharm Biotechnol *17*, 1213–1221.

Barone, D., Cito, L., Tommonaro, G., Abate, A.A., Penon, D., De Prisco, R., et al. (2017). Antitumoral potential, antioxidant activity and carotenoid content of two Southern Italy tomato cultivars extracts: San Marzano and Corbarino. J. Cell. Physiol. *96*, 171.

Ben Jannet, S., Hymery, N., Bourgou, S., Jdey, A., Lachaal, M., Magné, C., and Ksouri, R. (2017). Antioxidant and selective anticancer activities of two Euphorbia species in human acute myeloid leukemia. Biomed. Pharmacother. *90*, 375–385.

Boyd, M.R., Paull, K.D., and Rubinstein, L.R. (1992). Data Display and Analysis Strategies for the NCI Disease-Oriented in Vitro Antitumor Drug Screen. In Cytotoxic Anticancer Drugs: Models and Concepts for Drug Discovery and Development, (Boston, MA: Springer US), pp. 11–34.

Boyd, M.R., and Paull, K.D. (1995). Some practical considerations and applications of the national cancer institute in vitro anticancer drug discovery screen. Drug Development Research *34*, 91–109.

Cabrera, A.R., Espinosa-Bustos, C., Faúndez, M., Meléndez, J., Jaque, P., Daniliuc, C.G., et al. (2017). New imidoyl-indazole platinum (II) complexes as potential anticancer agents: Synthesis, evaluation of cytotoxicity, cell death and experimental-theoretical DNA interaction studies. J. Inorg. Biochem. *174*, 90–101.

Esposito, T., Sansone, F., Franceschelli, S., Del Gaudio, P., Picerno, P., Aquino, R.P., and Mencherini, T. (2017). Hazelnut (Corylus avellana L.) Shells Extract: Phenolic Composition, Antioxidant Effect and Cytotoxic Activity on Human Cancer Cell Lines. Int J Mol Sci *18*, 392.

Finlay, G.J., and Baguley, B.C. (1984). The use of human cancer cell lines as a primary screening system for antineoplastic compounds. Eur J Cancer Clin Oncol *20*, 947–954.

Fiorentino, F.P., Tokgün, E., Solé-Sánchez, S., Giampaolo, S., Tokgun, O., Jauset, T., et al. (2016). Growth suppression by MYC inhibition in small cell lung cancer cells with TP53 and RB1 inactivation. Oncotarget *7*, 31014–31028.

Hamed, M.M., Darwish, S.S., Herrmann, J., Abadi, A.H., and Engel, M. (2017). First Bispecific Inhibitors of the Epidermal Growth Factor Receptor Kinase and the NF-κB Activity As Novel Anticancer Agents. J. Med. Chem. *60*, 2853–2868.

Horvath, P., Aulner, N., Bickle, M., Davies, A.M., Del Nery, E., Ebner, D., et al. (2016). Screening out irrelevant cell-based models of disease. Nat Rev Drug Discov *15*, 751–769.

Indovina, P., Casini, N., Forte, I.M., Garofano, T., Cesari, D., Iannuzzi, C.A., et al. (2017). SRC Family Kinase Inhibition in Ewing Sarcoma Cells Induces p38 MAP Kinase-Mediated Cytotoxicity and Reduces Cell Migration. J. Cell. Physiol. *232*, 129–135.

Kato, F., Fiorentino, F.P., Alibés, A., Perucho, M., Sanchez-Cespedes, M., Kohno, T., and Yokota, J. (2016). MYCL is a target of a BET bromodomain inhibitor, JQ1, on growth suppression efficacy in small cell lung cancer cells. Oncotarget *7*, 77378–77388.

Koul, M., Kumar, A., Deshidi, R., Sharma, V., Singh, R.D., Singh, J., et al. (2017). Cladosporol A triggers apoptosis sensitivity by ROS-mediated autophagic flux in human breast cancer cells. BMC Cell Biol. *18*, 26.

Lukinavičius, G., Blaukopf, C., Pershagen, E., Schena, A., Reymond, L., Derivery, E., et al. (2015).

SiR-Hoechst is a far-red DNA stain for live-cell nanoscopy. Nat Commun *6*, 8497.

Marchesi, I., Sanna, L., Fais, M., Fiorentino, F.P., Giordano, A., and Bagella, L. (2017). 12-O-Tetradecanoylphorbol-13-acetate and EZH2 inhibition: a novel approach for promoting myogenic differentiation in embryonal rhabdomyosarcoma cells. J. Cell. Physiol.

Mathema, V.B., Chaijaroenkul, W., Karbwang, J., and Na-Bangchang, K. (2017). Growth inhibitory effect of β-eudesmol on cholangiocarcinoma cells and its potential suppressive effect on heme oxygenase-1 production, STAT1/3 activation, and NF-κB downregulation. Clin. Exp. Pharmacol. Physiol.

Menderes, G., Bonazzoli, E., Bellone, S., Black, J.D., Lopez, S., Pettinella, F., et al. (2017). Efficacy of neratinib in the treatment of HER2/neu-amplified epithelial ovarian carcinoma in vitro and in vivo. Medical Oncology *34*, 7.

Moffat, J.G., Rudolph, J., and Bailey, D. (2014). Phenotypic screening in cancer drug discovery — past, present and future. Nat Rev Drug Discov *13*, 588–602.

Mukunthan, K.S., Satyan, R.S., and Patel, T.N. (2017). Pharmacological evaluation of Phytochemicals from South Indian Black Turmeric (Curcuma caesia Roxb.) to target Cancer apoptosis. J Ethnopharmacol *209*, 82–90.

Muñoz, M., Rosso, M., and Coveñas, R. (2017). The NK-1 receptor antagonist L-732,138 induces apoptosis in human gastrointestinal cancer cell lines. Pharmacol Rep *69*, 696–701.

Nieddu, V., Pinna, G., Marchesi, I., Sanna, L., Asproni, B., Pinna, G.A., et al. (2016). Synthesis and Antineoplastic Evaluation of Novel Unsymmetrical 1,3,4-Oxadiazoles. J. Med. Chem. *59*, 10451–10469.

Pau, A., Murineddu, G., Asproni, B., Murruzzu, C., Grella, G.E., Pinna, G.A., et al. (2009). Synthesis and Cytotoxicity of Novel Hexahydrothienocycloheptapyridazinone Derivatives. Molecules *14*, 3494–3508.

Potenza, N., Mosca, N., Zappavigna, S., Castiello, F., Panella, M., Ferri, C., et al. (2017). MicroRNA-125a-5p Is a Downstream Effector of Sorafenib in Its Antiproliferative Activity Toward Human Hepatocellular Carcinoma Cells. J. Cell. Physiol. *232*, 1907–1913.

Ravi, M., Ramesh, A., and Pattabhi, A. (2017). Human Brain Malignant Glioma (BMG-1) 3D Aggregate Morphology and Screening for Cytotoxicity and Anti-Proliferative Effects. J. Cell. Physiol. *232*, 685–690.

Rello-Varona, S., Herrero-Martín, D., López-Alemany, R., Muñoz-Pinedo, C., and Tirado, O.M. (2015). "(Not) all (dead) things share the same breath": identification of cell death mechanisms in anticancer therapy. Cancer Research *75*, 913–917.

Rimoldi, I., Facchetti, G., Lucchini, G., Castiglioni, E., Marchianò, S., and Ferri, N. (2017). In vitro anticancer activity evaluation of new cationic platinum(II) complexes based on imidazole moiety. Bioorg. Med. Chem. *25*, 1907–1913.

Said, M., Brouard, I., Quintana, J., and Estévez, F. (2017). Antiproliferative activity and apoptosis induction by 3′,4′-dibenzyloxyflavonol on human leukemia cells. Chemico-Biological Interactions *268*, 13–23.

Selby, M., Delosh, R., Laudeman, J., Ogle, C., Reinhart, R., Silvers, T., et al. (2017). 3D Models of the NCI60 Cell Lines for Screening Oncology Compounds. SLAS Discov *22*, 473–483.

Venkataramana Reddy, P.O., Mishra, S., Tantak, M.P., Nikhil, K., Sadana, R., Shah, K., and

Kumar, D. (2017). Design, synthesis and in vitro cytotoxicity studies of novel β-carbolinium bromides. Bioorg. Med. Chem. Lett. *27*, 1379–1384.

Wehbe, M., Lo, C., Leung, A.W.Y., Dragowska, W.H., Ryan, G.M., and Bally, M.B. (2017). Copper (II) complexes of bidentate ligands exhibit potent anti-cancer activity regardless of platinum sensitivity status. Invest New Drugs *24*, 1529–1529.

Yoshida, M., Hoshi, A., Kuretani, K., Kanai, T., and Ichino, M. (1975). Action of 5-fluorocyclocytidine on cultured L-5178Y cells. Gan *66*, 561–564.

Zamora, A., Pérez, S.A., Rothemund, M., Rodríguez, V., Schobert, R., Janiak, C., and Ruiz, J. (2017). Exploring the Influence of the Aromaticity on the Anticancer and Antivascular Activities of Organoplatinum(II) Complexes. Chemistry *23*, 5614–5625.

Zhu, G.-X., Cheng, P.-L., Goto, M., Zhang, N., Morris-Natschke, S.L., Hsieh, K.-Y., et al. (2017). Design, synthesis and potent cytotoxic activity of novel 7-(N-[(substituted-sulfonyl)piperazinyl]-methyl)-camptothecin derivatives. Bioorg. Med. Chem. Lett. *27*, 1750–1753.

Table 1. Proliferation rate and parameter values of etoposide-treated A549 cells (biological replicates with mean ± standard deviation)

		Etoposide treatment (hours)			
		24	**48**	**72**	**Δ****
Cell proliferation in untreated samples	1st	1.84	3.89	7.59	-
	2nd	1.84	3.35	6.23	-
	3rd	1.64	3.31	5.55	-
	μ ± σ	**1.77 ± 0.12**	**3.52 ± 0.33**	**6.46 ± 1.04**	**-**
	CV (%)	***7%***	***9%***	***16%***	
Population doublings in untreated samples	1st	0.88	1.96	2.92	-
	2nd	0.88	1.74	2.64	-
	3rd	0.71	1.73	2.47	-
	μ ± σ	**0.82 ± 0.10**	**1.81 ± 0.13**	**2.68 ± 0.23**	-
	CV (%)	***12%***	***7%***	***9%***	-
IC_{50} (μM)	1st	18.20	1.18	0.60	-49.1%
	2nd	24.67	1.31	0.55	-57.8%
	3rd	52.02*	1.28	0.56	-56.2%
	μ ± σ	**31.63 ± 17.95**	**1.26 ± 0.07**	**0.57 ± 0.03**	**-54.4% ± 4.6%**
	CV (%)	***57%***	***6%***	***5%***	-
GI_{50} (μM)	1st	1.10	0.53	0.41	-22.2%
	2nd	1.00	0.52	0.38	-26.7%
	3rd	1.64	0.61	0.45	-25.8%
	μ ± σ	**1.25 ± 0.35**	**0.55 ± 0.05**	**0.42 ± 0.03**	**-24.9% ± 2.4%**
	CV (%)	***28%***	***9%***	***7%***	**-**
RD_{50} (μM)	1st	1.21	0.65	0.61	-6.5%
	2nd	1.02	0.58	0.49	-16.6%
	3rd	1.15	0.58	0.51	-12.5%
	μ ± σ	**1.13 ± 0.1**	**0.61 ± 0.04**	**0.54 ± 0.07**	**-11.9% ± 5.1%**
	CV (%)	***9%***	***7%***	***13%***	**-**
TGI (μM)	1st	11.89	5.66	5.60	-1.0%
	2nd	13.23	5.65	5.48	-3.0%
	3rd	14.23	5.81	4.10	-29.3%
	μ ± σ	**13.11 ± 1.17**	**5.71 ± 0.09**	**5.06 ± 0.83**	**-11.1% ± 15.8%**
	CV (%)	***9%***	***2%***	***16%***	**-**
RD_0 (μM)	1st	11.40	7.98	9.60	+20.3%
	2nd	12.64	7.42	8.72	+17.5%
	3rd	8.66	4.92	4.35	-11.6%
	μ ± σ	**10.90 ± 2.04**	**6.78 ± 1.63**	**7.56 ± 2.81**	**8.7% ± 17.7%**
	CV(%)	***19%***	***24%***	***37%***	**-**

μ: mean value of the three biological replicates

σ: standard deviation

CV: Coefficient of variation (σ/μ)

***out of scale**

****(72hr/48 hr)-1**

Table 2. Proliferation rate and parameter values of etoposide-treated PC3 cells (biological replicates with mean ± standard deviation)

		Etoposide treatment (hours)			
		24	**48**	**72**	**Δ****
Cell proliferation in untreated samples	1st	1.59	2.60	3.88	-
	2nd	1.62	2.52	3.54	-
	3rd	1.67	2.70	4.31	-
	μ ± σ	**1.63 ± 0.05**	**2.61 ± 0.09**	**3.91 ± 0.39**	-
	CV (%)	***3%***	***3%***	***10%***	
Population doublings in untreated samples	1st	0.66	1.38	1.95	-
	2nd	0.69	1.33	1.82	-
	3rd	0.74	1.43	2.11	-
	μ ± σ	**0.70 ± 0.04**	**1.38 ± 0.05**	**1.96 ± 0.14**	-
	CV (%)	***6%***	***4%***	***7%***	
IC_{50} (μM)	1st	>10*	6.18	3.46	-44.0%
	2nd	>10*	7.26	5.12	-29.4%
	3rd	>10*	5.51	3.21	-41.8%
	μ ± σ	**>10**	**6.32 ± 0.88**	**3.93 ± 1.04**	**-38.4% ± 7.9%**
	CV (%)	**-**	***14%***	***26%***	**-**
GI_{50} (μM)	1st	6.32	2.56	2.05	-19.5%
	2nd	4.77	3.39	3.41	+0.6%
	3rd	2.58	2.42	2.20	-9.4%
	μ ± σ	**4.56 ± 1.88**	**2.79 ± 0.53**	**2.55 ± 0.75**	**-7.6% ± 9.5%**
	CV (%)	***41%***	***19%***	***29%***	**-**
RD_{50} (μM)	1st	4.20	2.42	2.19	-9.4%
	2nd	4.09	3.33	3.54	+6.3%
	3rd	2.12	2.44	2.46	+0.5%
	μ ± σ	**3.47 ± 1.17**	**2.73 ± 0.52**	**2.72 ± 0.71**	**-0.9% ± 4.5%**
	CV (%)	***34%***	***19%***	***26%***	**-**

μ: mean value of the three biological replicates

σ: standard deviation

CV: Coefficient of variation (σ/μ)

***out of scale**

****(72hr/48 hr)-1**

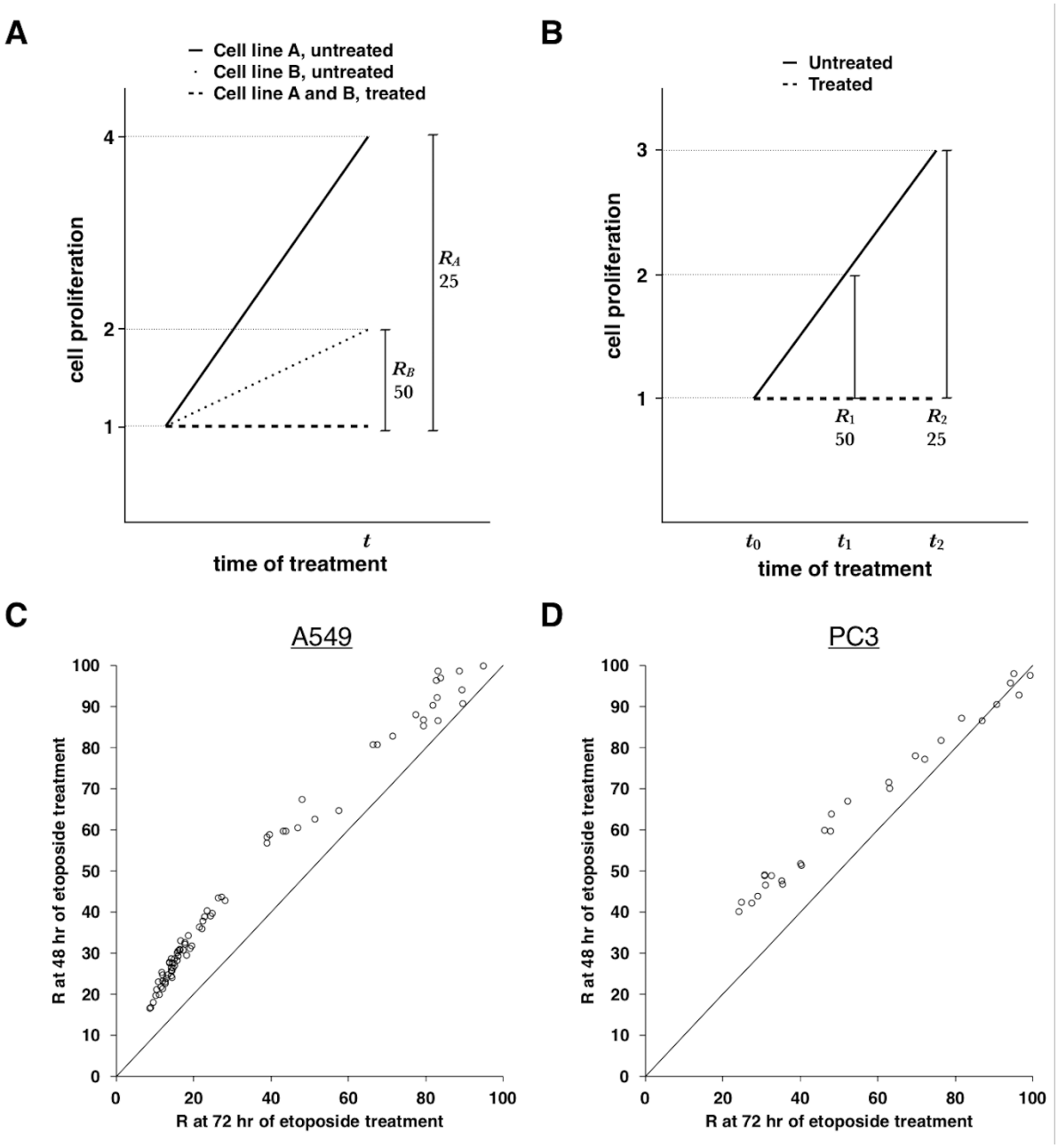

Figure 1

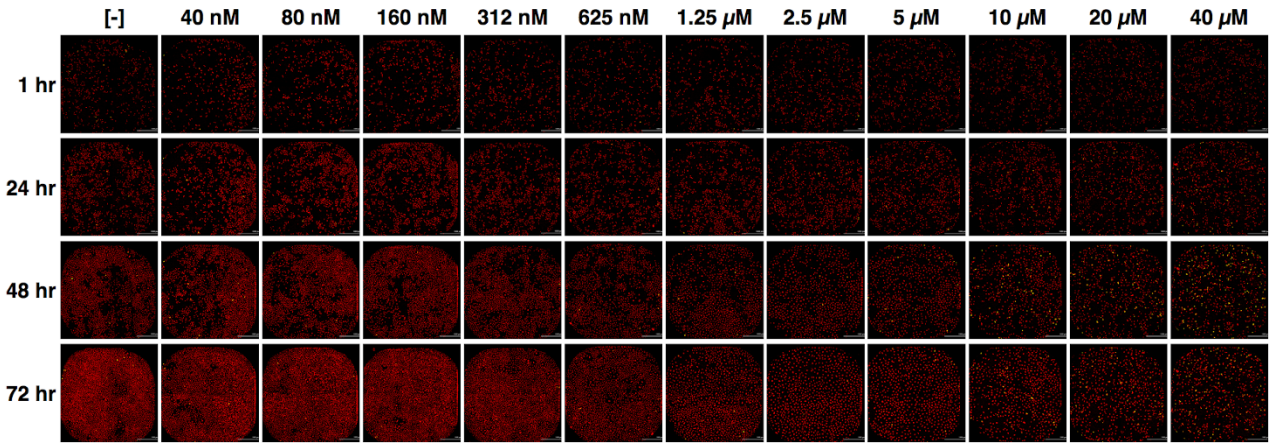

Figure 2

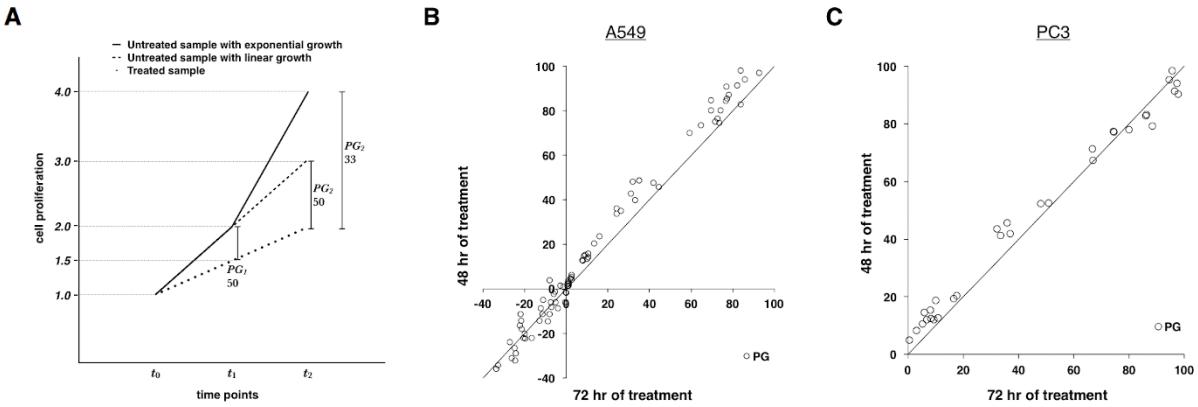

Figure 3

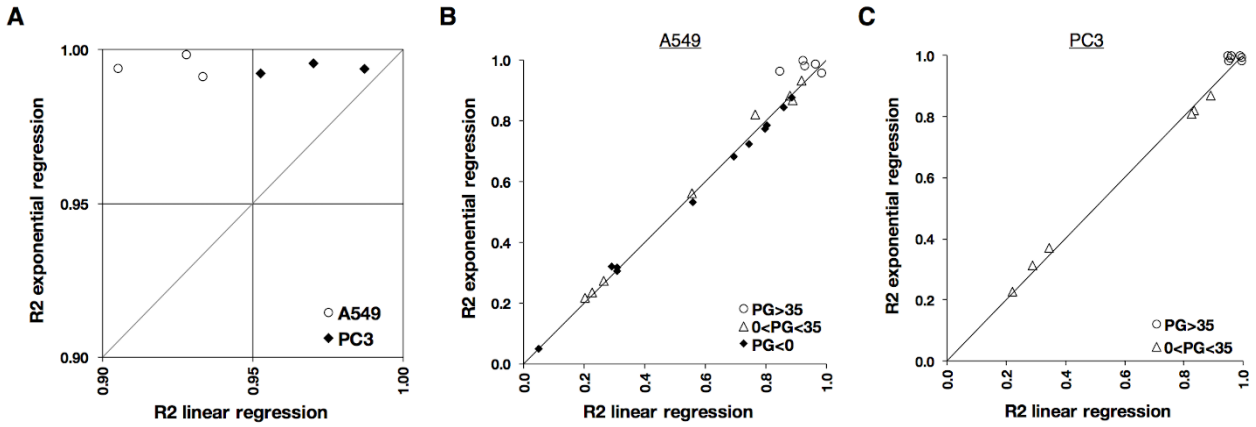

Figure 4

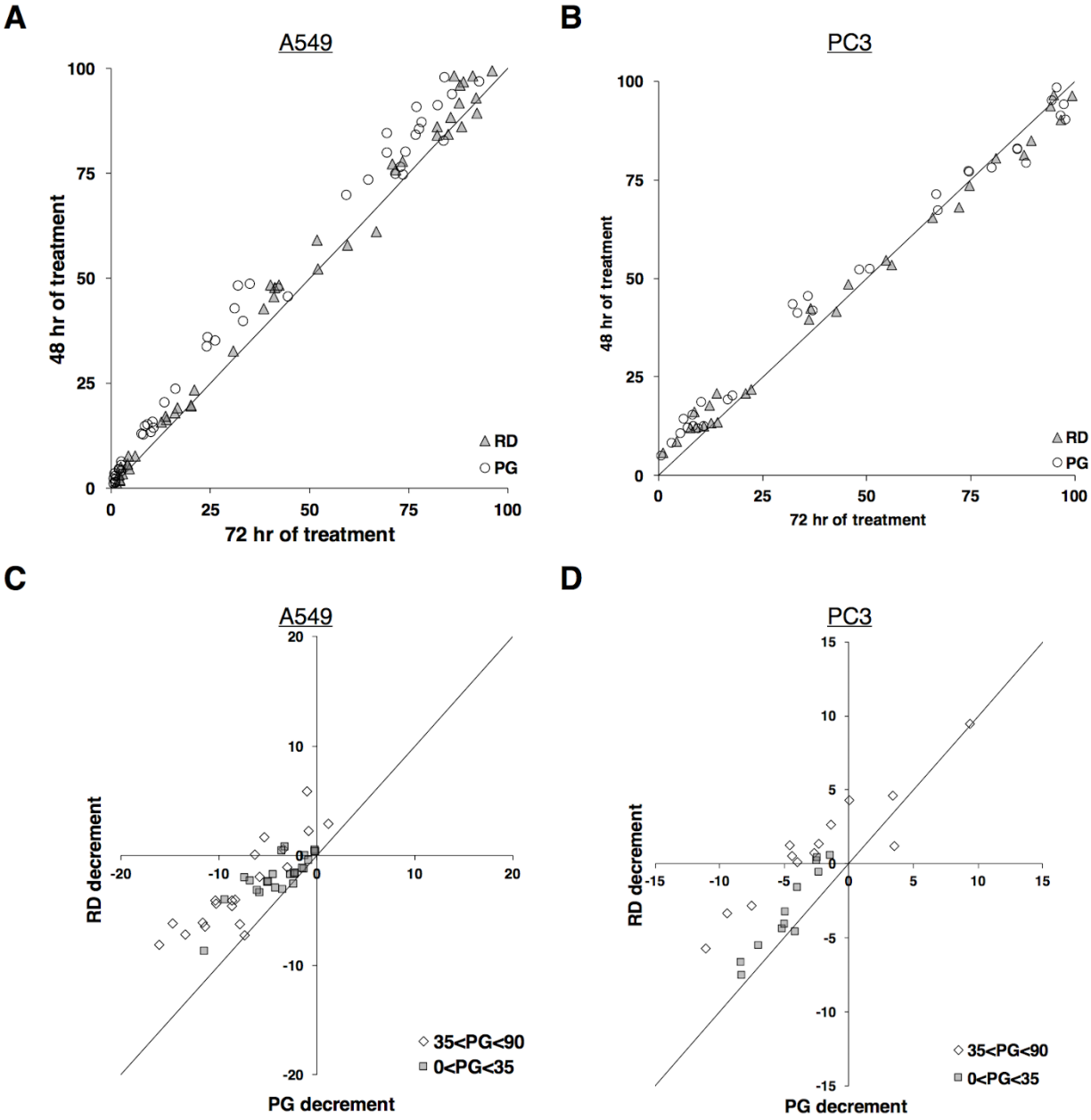

Figure 5